Available online at www.sciencedirect.com
ScienceDirect
International Journal of Heat and Fluid Flow 29 (2008) 540–544
International Journal of HEAT AND FLUID FLOW
www.elsevier.com/locate/ijhff

# Numerical study of laminar fluid flow in a curved elliptic duct with internal fins

P.K. Papadopoulos *, P.M. Hatzikonstantinou

*Department of Engineering Science, University of Patras, GR 26500 Patras, Greece*

Received 30 November 2006; received in revised form 14 October 2007; accepted 8 November 2007
Available online 8 January 2008

**Abstract**

The fully developed laminar incompressible flow inside a curved duct of elliptical cross-section with four thin, internal longitudinal fins is studied using the improved CVP method. We present numerical results for the friction factor and an investigation of the effect of the fin height and the Dean number on the flow. It is found that the friction factor increases for large fins and for high Dean numbers and that in some cases, it has a strong dependence on the cross-sectional aspect ratio. The thermal results show that the heat transfer rate is enhanced by the internal fins and that it depends on the aspect ratio.


*Keywords:* Laminar flow; Curved elliptic duct; Internal fins

## 1. Introduction

Internal flows are of primary interest in engineering. Special attention has been given to ducts of elliptical cross-section which have increased heat transfer rates compared to circular pipes (Sakalis and Hatzikonstantinou, 2002) and relevant studies have been published by Topakoglu and Ebadian (1985) and by Dong and Ebadian (1991).

In the present work we use the CVP method (Papadopoulos and Hatzikonstantinou, 2004) to investigate the fully developed incompressible flow inside a curved duct of elliptical cross-section with four internal fins. Extensive results of the Dean number, the Nusselt number and the friction factor are produced over a wide range of values of the curvature, the axial pressure gradient and the aspect ratio of the cross-section for various fin heights.

## 2. Analysis

We consider a toroidal coordinate system as shown in Fig. 1. The governing equations are transformed to a generalized $(\xi,\eta)$ boundary system, (Thompson et al., 1974) and we impose orthogonality conditions for the grid on the boundaries (Thomas and Middlecoff, 1980). The non-dimensional variables used, are defined by the relations

$$\begin{aligned} &x,y,z=(X,Y,Z)/D_{\mathrm{h}}, \quad \kappa=D_{\mathrm{h}}/R,\\ &u,v,w=(U,V,W)D_{\mathrm{h}}/v, \quad p=PD_{\mathrm{h}}^2/\rho v^2,\\ &\theta=(T-T_{\mathrm{reference}})/(T_{\mathrm{surface}}-T_{\mathrm{reference}}) \end{aligned} \tag{1}$$

where $D_{\mathrm{h}}$ is the hydraulic diameter and $P,\rho,v,T$ are the dimensional pressure, the density, the kinematic viscosity and the temperature respectively. The relative fin height $H$ is defined as $H=H_a/a=H_b/b$. The governing equations expressed in the generalized coordinate system with the non-dimensional variables take the form:

Continuity equation

$$\frac{\partial\overline{U}}{\partial\xi}+\frac{\partial\overline{V}}{\partial\eta}+J\kappa Cu=0 \tag{2}$$

* Corresponding author. Tel./fax: +30 2610997710.
*E-mail address:* p.papadopoulos@des.upatras.gr (P.K. Papadopoulos).

0142-727X/$ - see front matter © 2007 Elsevier Inc. All rights reserved.
doi:10.1016/j.ijheatfluidflow.2007.11.003

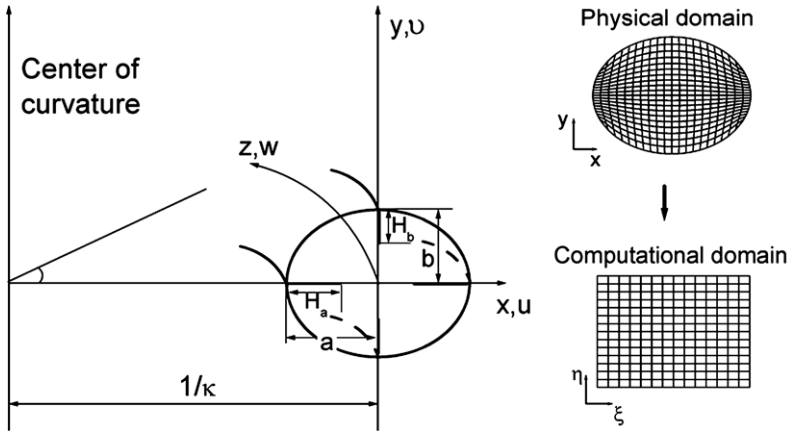


Fig. 1. Geometry and coordinate system.

$u$-momentum equation

$$\frac{\partial(\overline{U}u)}{\partial\xi}+\frac{\partial(\overline{V}u)}{\partial\eta}=\frac{1}{J}\left(\alpha\frac{\partial^2u}{\partial\xi^2}-2\beta\frac{\partial^2u}{\partial\xi\partial\eta}+\gamma\frac{\partial^2u}{\partial\eta^2}\right)-\left(\frac{\partial p}{\partial\xi}y_\eta-\frac{\partial p}{\partial\eta}y_\xi\right)+\kappa C\left(\frac{\partial u}{\partial\xi}y_\eta-\frac{\partial u}{\partial\eta}y_\xi\right)+J\kappa C(w^2-u^2)-J(\kappa C)^2u \tag{3}$$

$v$-momentum equation

$$\frac{\partial(\overline{U}v)}{\partial\xi}+\frac{\partial(\overline{V}v)}{\partial\eta}=\frac{1}{J}\left(\alpha\frac{\partial^2v}{\partial\xi^2}-2\beta\frac{\partial^2v}{\partial\xi\partial\eta}+\gamma\frac{\partial^2v}{\partial\eta^2}\right)+\left(\frac{\partial p}{\partial\xi}x_\eta-\frac{\partial p}{\partial\eta}x_\xi\right)+\kappa C\left(\frac{\partial v}{\partial\xi}y_\eta-\frac{\partial v}{\partial\eta}y_\xi\right)-J\kappa Cuv \tag{4}$$

$w$-momentum equation

$$\frac{\partial(\overline{U}w)}{\partial\xi}+\frac{\partial(\overline{V}w)}{\partial\eta}=\frac{1}{J}\left(\alpha\frac{\partial^2w}{\partial\xi^2}-2\beta\frac{\partial^2w}{\partial\xi\partial\eta}+\gamma\frac{\partial^2w}{\partial\eta^2}\right)-JC\frac{\mathrm{d}p_a}{\mathrm{d}z}+\kappa C\left(\frac{\partial w}{\partial\xi}y_\eta-\frac{\partial w}{\partial\eta}y_\xi\right)-2J\kappa Cuw-J(\kappa C)^2w \tag{5}$$

Energy equation

$$\overline{U}\frac{\partial\theta}{\partial\xi}+\overline{V}\frac{\partial\theta}{\partial\eta}=\frac{1}{Pr}\left[\frac{1}{J}\left(\alpha\frac{\partial^2\theta}{\partial\xi^2}-2\beta\frac{\partial^2\theta}{\partial\xi\partial\eta}+\gamma\frac{\partial^2\theta}{\partial\eta^2}\right)+\kappa C\left(\frac{\partial\theta}{\partial\xi}y_\eta-\frac{\partial\theta}{\partial\eta}y_\xi\right)\right] \tag{6}$$

where $C=1/(\kappa x+1)$ and

$$\overline{U}=uy_\eta-vx_\eta,\quad \overline{V}=vx_\xi-uy_\xi,\quad J=x_\xi y_\eta-x_\eta y_\xi$$
$$\alpha=x_\eta^2+y_\eta^2,\quad \beta=x_\xi x_\eta+y_\xi y_\eta,\quad \gamma=x_\xi^2+y_\xi^2 \tag{7}$$

The pressure splitting technique (Fletcher, 1991) has been implemented and $\mathrm{d}p_a/\mathrm{d}z$ denotes the axial pressure gradient.

At the boundaries (duct wall and fins) we use the no slip condition for the velocity and the constant temperature condition. The mean axial velocity, which in the present non-dimensional form coincides with the Reynolds number, the Dean number and the product of the friction factor $f$ with the Reynolds number are given by the formulae

$$Re\equiv\bar{w}=\frac{\int_A w\mathrm{d}A}{\int_A\mathrm{d}A},\quad De=Re\sqrt{\kappa},$$
$$fRe=-\left(\frac{\mathrm{d}p_a}{\mathrm{d}z}\right)/(2\bar{w}) \tag{8}$$

The dimensionless bulk temperature $\theta_b$, the Nusselt number and the Peclet number are

$$\theta_b=\frac{\int_A w\theta\mathrm{d}A}{\int_A w\mathrm{d}A},\quad Nu=\frac{1}{4(1-\theta_b)}\frac{\overline{w}}{\bar{w}}Pe\frac{\overline{\partial\theta}}{\partial z},\quad Pe=RePr \tag{9}$$

## 3. Numerical implementation

The governing equations were solved on a $48\times24$ mesh with the CVP method. Convergence was declared when the following criterion was satisfied at all the nodes

$$\left\|\phi_{ij}^{k+1}-\phi_{i\xi}^{k}\right\|_\infty\Big/\left\|\phi_{ij}^{k+1}\right\|_\infty\leqslant10^{-5} \tag{10}$$

where $\phi$ stands for velocities $u,v,w$, the subscripts $i,j$ represent the grid nodes in the $\xi$ and $\eta$ coordinates and the superscript $k$ is the $k$th iteration.

In order to assure the accuracy of the present results, we present in Fig. 2a comparison of our results with the measurements of Mori and Nakayama (1965) for a curved duct of circular cross-section. The curvature of the duct is $\kappa=0.05$ and the flow is considered fully developed with $Re=2800$ in the first case Fig. 2a and $Re=4000$ in the second case Fig. 2b. It can be seen that the numerical results are in very good agreement with the experimental measurements. We also conduct a comparison with the numerical data for a finless curved elliptical duct of Dong and Ebadian (1991) who used the SIMPLE method. The compari-

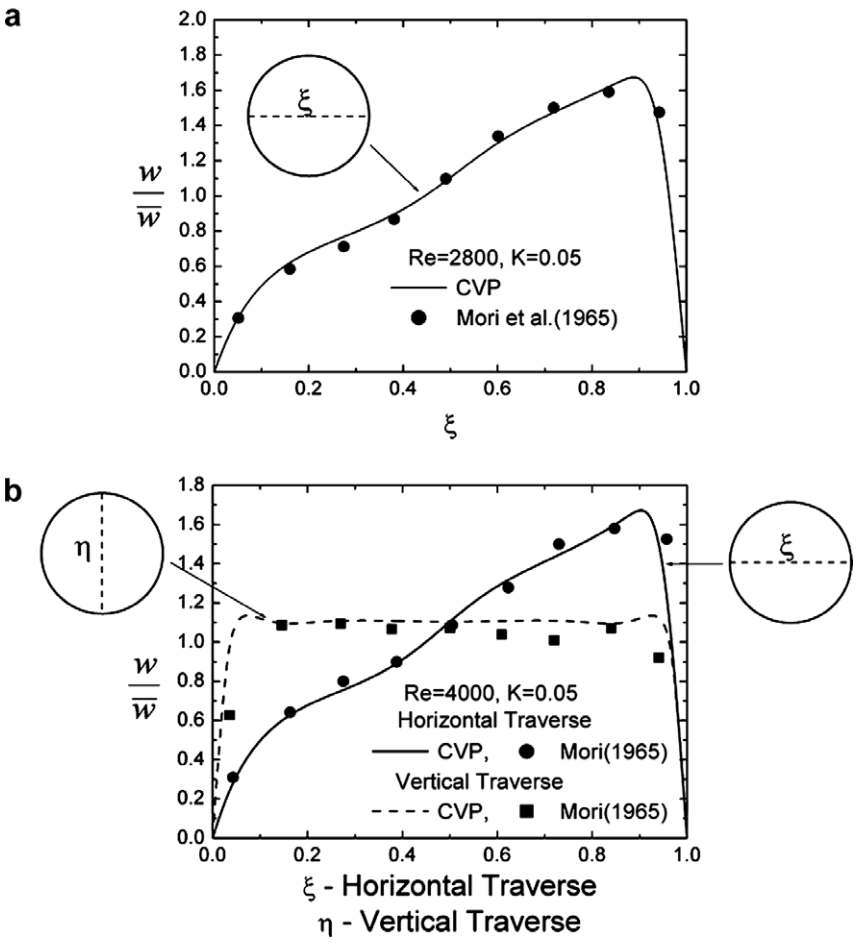


Fig. 2. Comparison between the present numerical results and experimental data from Mori and Nakayama (1965) for flow in a curved pipe with (a) $De = 626$ along the horizontal axis ($\eta = 0$) and (b) $De = 894$ along the horizontal ($\eta = 0$) and vertical ($\xi = 0$) axis.

Table 1
Comparison of numerical results of the present method with results of Dong and Ebadian (1991) for a curved finless duct

| $b/a$ | $dp_a/dz$ | $\kappa$ | $De_{present}$ | $De_{Dong}$ | % Divergence |
|---|---|---|---|---|---|
| 0.2 | $-8 \times 10^4$ | 0.01 | 162.0 | 158.1 | 2.47 |
| 0.5 | $-4 \times 10^3$ | 0.1 | 35.08 | 34.4 | 1.97 |
| 0.5 | $-1.1 \times 10^5$ | 0.01 | 193.38 | 192.1 | 0.66 |
| 0.8 | $-4 \times 10^3$ | 0.25 | 51.24 | 49.7 | 3.10 |
| 0.8 | $-1.1 \times 10^5$ | 0.01 | 199.12 | 194.1 | 2.59 |

son is presented in Table 1 and it shows a very good agreement of the Dean number values.

## 4. Results and discussion

The introduction of fins in the elliptic duct affects significantly the behavior of the flow. Figs. 3a–d show contour plots of the stream function $\Psi$ of the transversal velocities and contour plots of the axial velocity $w$ normalized by the mean axial velocity $\bar{w}$ in a duct of aspect ratio $b/a = 0.5$ and $\kappa = 0.1$. The plots correspond to $De = 49$ in Fig. 3a, $De = 127$ in Fig. 3b and $De = 274$ in Fig. 3c for fin height $H = 0.5$ and to $De = 167.8$ in Fig. 3d, for fin height $H = 0.75$.

Table 2 presents the quantities $De$ and $fRe$ for various curvatures, axial pressure gradients and fin heights in a duct of $b/a = 0.5$. The variation of $fRe$ shows a 6% average increase as the fin height changes form $H = 0$ to $H = 0.25$, 29.7% from $H = 0.25$ to $H = 0.5$ and 36.7% from $H = 0.5$ to 0.75. Another observation from Table 2 is that $fRe$ depends less on the curvature, as the fin height increases. For constant pressure gradient $dp_a/dz = -25000$ and for $H = 0.25$ there is a 30% decrease of $fRe$ as the curvature decreases from 0.25 to 0.01, while for $H = 0.75$ the decrease is only 2.5%.

A more general view of the elements that affect the friction factor can be obtained from Fig. 4. In this plot the friction factor product is plotted against the Dean number for axis ratios $b/a = 0.8$, 0.5, 0.2 and for fin heights $H = 0$, 0.25, 0.5, 0.75. The variation of $fRe$ with the Dean number is essentially linear with few exceptions mainly for low Dean numbers. Moreover, $fRe$ decreases as the b/a ratio decreases and the decrease is greater for higher fins. For the case of $H = 0.75$, it is observed that there is an approximate decrease of 4% for $fRe$ between aspect ratios

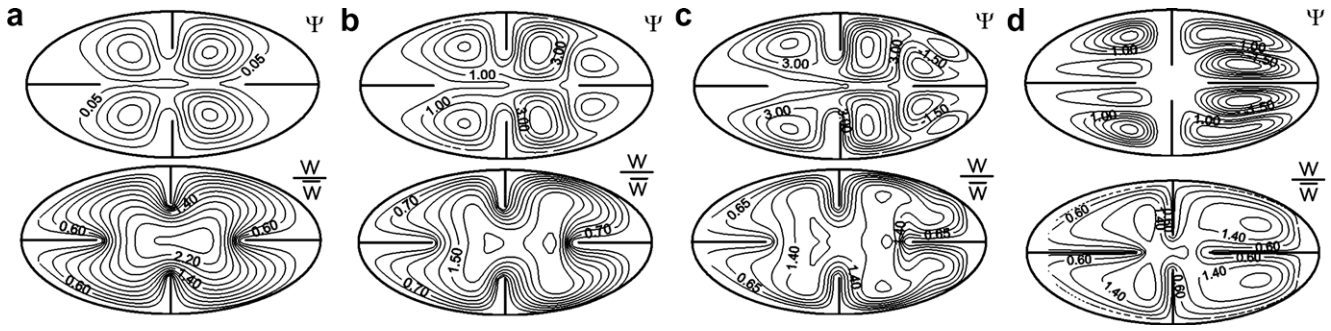


Fig. 3. Contour plots of the stream function $\Psi$ and the normalized axial velocity $w/\bar{w}$ for $b/a = 0.5$, $H = 0.5$ and $De = 49$, (b) $De = 127$, (c) $De = 274$, and for (d) $b/a = 0.5$, $H = 0.75$ and $De = 167.8$.

Table 2
Results for constant cross-section ratio $b/a = 0.5$

| $dp_a/dz$ | $H = 0$ | | $H = 0.25$ | | $H = 0.5$ | | $H = 0.75$ | |
|---|---|---|---|---|---|---|---|---|
| | *De* | *fRe* | *De* | *fRe* | *De* | *fRe* | *De* | *fRe* |
| *κ = 0.01* | | | | | | | | |
| $-4 \times 10^3$ | 11.6 | 17.2 | 8.8 | 22.5 | 5.1 | 39.0 | 2.9 | 68.0 |
| $-25 \times 10^3$ | 61.9 | 20.1 | 49.9 | 25.0 | 31.7 | 39.3 | 18.3 | 68.0 |
| $-80 \times 10^3$ | 151.4 | 26.4 | 127.4 | 31.3 | 91.5 | 43.6 | 58.4 | 68.3 |
| $-200 \times 10^3$ | 303.2 | 32.9 | 264.7 | 37.7 | 197.7 | 50.5 | 137.3 | 72.8 |
| *κ = 0.1* | | | | | | | | |
| $-4 \times 10^3$ | 35.0 | 18.0 | 27.5 | 22.9 | 16.2 | 39.0 | 9.3 | 67.9 |
| $-25 \times 10^3$ | 147.3 | 26.8 | 124.1 | 31.8 | 90.0 | 43.9 | 57.7 | 68.4 |
| $-80 \times 10^3$ | 354.4 | 35.6 | 312.4 | 40.4 | 237.5 | 53.2 | 167.1 | 75.6 |
| *κ = 0.25* | | | | | | | | |
| $-4 \times 10^3$ | 50.6 | 19.7 | 40.8 | 24.4 | 25.5 | 39.1 | 14.7 | 67.6 |
| $-25 \times 10^3$ | 203.9 | 30.6 | 176.5 | 35.3 | 131.8 | 47.4 | 89.5 | 69.8 |

$b/a = 0.8$ and $b/a = 0.5$ and of 23% between aspect ratios $b/a = 0.8$ and $b/a = 0.2$.

Fig. 5 shows the dependence of *Nu* on *De* for $Pr = 7$, aspect ratios $b/a = 0.8$ and $b/a = 0.5$ and various fin heights. The plot shows an initial region with a steep inclination which fades after a certain value of *De* for most fin heights. It is observed that there is an average 11% increase of *Nu* from $H = 0$ to $H = 0.25$, 15% from $H = 0.25$ to $H = 0.5$ and 84% from $H = 0.5$ to $H = 0.75$. Taking into account the corresponding variation for *fRe*, it is obtained that small fins can enhance the heat transfer rates without increasing the friction losses significantly and that large fins

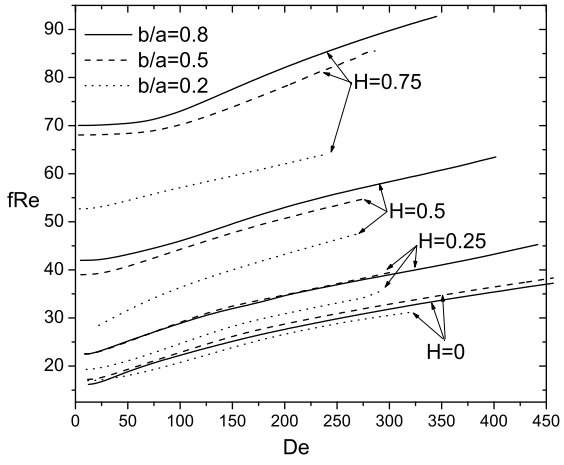


Fig. 4. Friction factor product *fRe* vs. *De* for aspect ratios $b/a = 0.8, 0.5, 0.2$ and fin heights $H = 0, 0.25, 0.5, 0.75$.

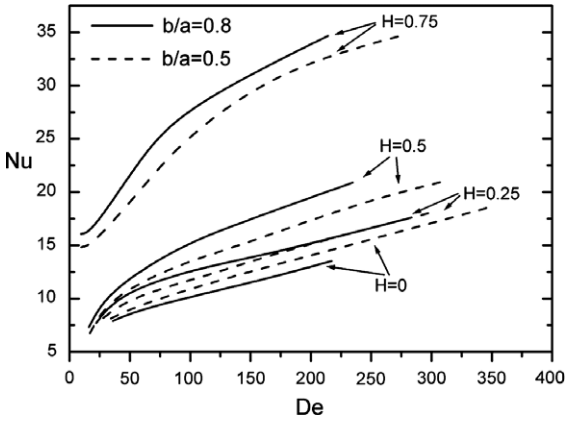


Fig. 5. Nusselt number variation with *De* for aspect ratios $b/a = 0.8, 0.5$ and fin heights $H = 0, 0.25, 0.5, 0.75$ and $Pr = 7$.

triple the Nusselt number compared to the finless case. Another observation is that there is a 5% decrease of $Nu$ as the aspect ratio decreases from $b/a = 0.8$ to $b/a = 0.5$ for large fins and 13% for medium fins. The opposite is observed for the finless case, where the duct with $b/a = 0.5$ achieves higher heat transfer rate than $b/a = 0.8$.

## 5. Conclusions

In the present investigation it has been found that the insertion of fins in a curved duct increases the friction factor product especially for high fins and that $fRe$ depends strongly on the Dean number. The friction factor product also decreases for low aspect ratio especially for large fins. Concerning the heat transfer rate, it is enhanced by the fins and the increase is maximum for aspect ratio $b/a = 0.5$.

## Acknowledgement

This work is part of "Karatheodoris" program, funded by the University of Patras Research Committee.

## References

Dong, Z.F., Ebadian, M.A., 1991. Numerical analysis of laminar flow in curved elliptic ducts. ASME J. Fluid Eng. 113, 555–562.

Fletcher, C.A.J., 1991Computational Techniques for Fluid Dynamics, vol. 2. Springer-Verlag, Berlin Heidelberg, pp. 273–277.

Mori, Y., Nakayama, W., 1965. Study on forced convective heat transfer in curved pipes. Int. J. Heat Mass Transfer 8, 67–82.

Papadopoulos, P.K., Hatzikonstantinou, P.M., 2004. Comparison of the CVP and the SIMPLE methods for solving internal incompressible flows. In: Topping, B.H.V., Mota Soares, C.A. (Eds.), Proceedings of the Fourth International Conference on Engineering Computational Technology. Civil-Comp Press, Stirling, Scotland.

Sakalis, V.D., Hatzikonstantinou, P.M., 2002. Thermally developing flow in elliptic ducts with axially variable wall temperature. Int. J. Heat Mass Transfer 45, 25–35.

Thomas, P.D., Middlecoff, J.F., 1980. Direct control of grid point distribution in meshes generated by elliptic equations. AIAA J. 18, 652–656.

Thompson, J.F., Thames, F., Mastin, C., 1974. Automatic numerical generation of body-fitted curvilinear coordinate system for field containing any number of arbitrary two-dimensional bodies. J. Comput. Phys. 15, 299–319.

Topakoglu, H.C., Ebadian, M.A., 1985. On the steady laminar flow of an incompressible viscous fluid in a curved pipe of elliptical cross-section. J. Fluid Mech. 158, 329–340.